Journal of Nonlinear Modeling and Analysis
Volume 7, Number 6, December 2025, 2349–2378
https://journal.global-sci.org/jnma
DOI:10.12150/jnma.2025.2349

Bifurcation Analysis of Predator-Prey Mathematical Model with Resource-Limited Growth and Predator Switching Behavior

Negeri Negese Wayesa[1,†], Legesa Lemecha Obsu[2] and Mohammed Yiha Dawed[3]

Abstract Ecology examines the interactions between organisms and their environment, with a particular focus on population dynamics, resource availability, and predator-prey relationships. This study presents a mathematical model designed to investigate the interactions between two prey populations, one in an unprotected region and the other in a protected region, along with a predator population and shared resource availability. The model employs nonlinear differential equations to capture processes such as prey growth, predation, and resource utilization. By identifying equilibrium points and conducting eigenvalue analysis, we assess the system's stability. Numerical simulations demonstrate a range of outcomes, including stable states, cyclic behavior, and population collapse, depending on ecological conditions (parametric values). Biologically, predator-prey coexistence equilibria may lose stability, shifting to extinction or dominance scenarios. This makes bifurcation point. Bifurcation analysis reveals how competition and predation impact stability, with critical points marking transitions between coexistence, oscillations, or extinction. These results underscore the intricate balance of ecological forces and emphasize the significance of resource management and conservation in preserving ecosystem stability.

Keywords Ecology, predator-prey model, resource availability, stability analysis, local bifurcation

MSC(2010) 34C23, 37C75, 34D20, 34D23, 37N25.

1. Introduction

Ecology, a discipline within biology, examines the distribution of organisms and their interactions with the environment and one another [1–3]. The evolution and growth of species are shaped by a range of factors, including population density, resource availability, interspecies interactions, and the ecological and environmental conditions of their habitats [4]. The incorporation of mathematical frameworks into

---

[†] the corresponding author.
Email address:negerirome@gmail.com (Negeri Negese Wayesa), legese.lemecha@astu.edu.et (Legese Lemecha Obsu), mohammedyiha2017@gmail.com (Mohammed Yiha Dawed)
[1] Department of Mathematics, Bule Hora University, Bule Hora, Ethiopia.
[2] Department of Applied Mathematics, Adama Science and Technology University, Adama, Etiopia.
[3] Department of Mathematics, Hawassa University, Hawassa, Etiopia.

ecological research has given rise to the field of mathematical ecology, which utilizes mathematical models and equations to describe and predict the temporal dynamics of interacting species. The study of predator-prey interactions has been a fundamental area of ecological research, with mathematical modeling playing a crucial role in understanding population dynamics and ecosystem stability [1,5]. Classical models, such as the Lotka-Volterra equations, provide foundational insights but are often limited in their ability to capture the complexity of real-world ecosystems [4, 6, 7]. Natural habitats are heterogeneous, with prey distributed across areas of varying predation risk and resource availability, such as reserved (low risk, resource-rich) and unreserved (high risk, resource-limited) zones [8]. Resources play a crucial role in shaping prey distribution, reproduction, and survival, further influencing predator-prey dynamics. Classical models like Lotka-Volterra assume homogeneous environments and linear dynamics, oversimplifying real ecosystems [9, 10]. As reported in [11–13] the Holling Type-II functional response improved upon this by incorporating saturating predation rates but overlooked spatial heterogeneity, resource limitation, and predator switching where predators shift to abundant prey to optimize energy intake. Spatially explicit models better capture ecological complexity, emphasizing the role of reserved zones and resource distribution in stabilizing prey populations and informing conservation strategies. Additionally, resource availability, a critical factor influencing prey reproduction and predator survival, is inherently dynamic and subject to environmental fluctuations [14, 15]. To better understand these interactions, models must incorporate spatial structure, resource dynamics, and predator-prey interactions. This study extends traditional models by introducing a framework where prey are divided into unreserved and reserved regions, predators roam freely, and resource availability fluctuates dynamically, offering a more realistic representation of ecological systems. The main challenge is understanding how spatially structured habitats and dynamic resources influence predator-prey interactions and population stability. Traditional models, assuming homogeneous environments and constant resources, fail to capture the complexity of natural systems, limiting their predictive power. This study addresses this gap by developing a mathematical model that integrates spatial heterogeneity, predator-prey dynamics, and resource variability to explore these interactions in structured ecological contexts.

Existing predator-prey models are constrained by simplifying assumptions that overlook critical aspects of real world ecosystems [16, 17]. These include spatial heterogeneity, where reserved zones lower predation risk and unreserved zones face higher predation [18], as well as temporal resource dynamics affecting prey growth and predator survival. Traditional models also overlook non-linear interactions between prey across regions and predators moving through the landscape. To address these gaps, this study introduces a comprehensive mathematical model incorporating spatially structured prey, dynamic resources, and predator-prey interactions. This framework aims to enhance understanding of ecological dynamics, improve population predictions, and support conservation strategies in structured, dynamic habitats.

2. Mathematical model assumption

This document presents a prey-predator model that integrates logistic resource dynamics and a protected prey population. The model captures the interactions between unprotected prey, protected prey, predators, and resources. We assume that the predation term accounts for preference toward unprotected prey, but allows switching to protected prey as they become more available. Let the predation rate on each prey type be a function of the relative abundance of unprotected N_u and protected prey N_r. We assume that predators preferentially consume unprotected prey, but they can switch to protected prey based on their relative abundance. When unprotected prey are abundant, predators primarily consume them [19, 20]. However, when unprotected prey become scarce, they switch to protected prey [21], optimizing their diet based on resource availability. Incorporating this behavior into mathematical models improves ecosystem representation by capturing predator foraging strategies. This switching mechanism helps balance prey populations, preventing overexploitation while sustaining predators. A common approach to model this is using a weighted ratio to reflect predator preference. The term $r_uN_u\left(1-\frac{N_u}{K_u}\right)\frac{R}{R_{\max}}$, represents the logistic growth of the prey population in the unprotected region, regulated by intrinsic growth rate (r_u) and carrying capacity (K_u), while being further influenced by resource availability (R), scaled by the maximum resource limit $(R_{\max})$, ensuring that prey reproduction depends on available of resource. The term $r_rN_r\left(1-\frac{N_r}{K_r}\right)\frac{R}{R_{\max}}$, represents the prey population in the protected region grows logistically with intrinsic growth rate (r_r), modulated by the available resource. The term $r_RR\left(1-\frac{R}{R_{\max}}\right)$, represents resource availability follows logistic growth model with growth rate (r_R) and maximum capacity $(R_{\max})$. For instance, the proportion of unprotected prey in the predator's diet could be modeled by a ratio $\frac{N_u}{N_r+N_u}$. Here, $\frac{N_u}{N_r+N_u}$ represents the preference for unprotected prey (if N_r is large relative to N_u, the predator switches to protected prey). Further, r_c is still the growth rate of predators, but now the predation pressure depends on the relative proportions of the two prey types. $\frac{cN_uN_c}{N_r+N_u}$ represents the reduced predation on unprotected prey due to the predator's switching behavior. The predation term for protected prey is proportional to $\frac{N_r}{N_r+N_u}$ and $\frac{cN_rN_c}{N_r+N_u}$ accounts for the switching behavior of predators consuming protected prey when unprotected prey are scarce. Further we assume that the growth of both unprotected and protected prey is now directly linked to the relative availability of resources. This means the prey growth is scaled by the factor $\frac{R}{R_{max}}$, which represents the proportion of available resources compared to the maximum capacity R_{max}. When resources are scarce $R \ll R_{max}$, prey growth will slow down.

The terms $-\alpha_uN_uR$ and $-\alpha_rN_rR$ indicate the consumption of r by the unprotected and protected prey populations, respectively. This consumption reduces the available resource based on the population sizes of N_u and N_r and their specific consumption rates, α_u and α_r. Thus, the interaction between predation, competition, and resource availability shapes the system's stability and bahavior.

Considering the above assumptions, the model system of equations governing the dynamics of the prey-predator-resource system is given by:

$$\begin{cases} \frac{dN_u(t)}{dt} = r_uN_u(t)\left(1-\frac{N_u(t)}{K_u}\right)\frac{R(t)}{R_{\max}} - c\frac{N_u(t)N_c(t)}{N_u(t)+N_r(t)}, \\ \frac{dN_r(t)}{dt} = r_rN_r(t)\left(1-\frac{N_r(t)}{K_r}\right)\frac{R(t)}{R_{\max}} - c\frac{N_r(t)N_c(t)}{N_u(t)+N_r(t)}, \\ \frac{dN_c(t)}{dt} = r_c\left(\frac{N_u(t)N_c(t)}{N_u(t)+N_r(t)}\right) - dN_c(t), \\ \frac{dR(t)}{dt} = r_RR(t)\left(1-\frac{R(t)}{R_{\max}}\right) - \alpha_uN_u(t)R(t) - \alpha_rN_r(t)R(t), \end{cases} \tag{2.1}$$

with initial conditions

$$N_u(t_0) = N_{u_0} > 0, N_r(t_0) = N_{r_0} > 0, N_c(t_0) = N_{c_0} > 0, R(t_0) = R_0 > 0, 0 < c < 1.$$

The model presented above outlines the dynamics of a predator-prey system with two distinct prey populations and a shared resource. The first equation describes the dynamics of the prey population in the unprotected region, which interacts with both the predator and the resource availability. The second equation models the dynamics of the prey population in the protected region, incorporating natural mortality and predation effects, as well as resource dependence. The third equation focuses on the predator population, whose growth is influenced by its consumption of prey in both regions. Finally, the fourth equation represents the dynamics of the resource, considering its logistic growth and depletion due to consumption by both prey populations. Together, these equations illustrate the interactions and dependencies within the ecosystem.

The descriptions of the model variables and their parameters are presented in Table 2 along with their biological interpretations. The construction of dimensionless parameters, achieved by the algebraic manipulation of fundamental variables to yield unitless quantities, is an essential tool in applied mathematics, allowing for equation simplification, identification of governing parameters, and the application of similarity theory.

Thus, to nondimensionalize the model equation (2.1), we introduce the following dimensionless variables based on its natural scales:

$$n_u = \frac{N_u}{K_u}, \quad n_r = \frac{N_r}{K_r}, \quad n_c = \frac{N_c}{K_u}, \quad r = \frac{R}{R_{\max}}, \quad \tau = r_R t. \tag{2.2}$$

Substituting Equation (2.2) into (2.1), we express the derivatives in terms of the new variables:

$$\frac{dn_u}{d\tau} = \frac{dn_u}{dN_u}\frac{dN_u}{dt}\frac{dt}{d\tau}, \quad \frac{dn_r}{d\tau} = \frac{dn_r}{dN_r}\frac{dN_r}{dt}\frac{dt}{d\tau}, \quad \frac{dn_c}{d\tau} = \frac{dn_c}{dN_c}\frac{dN_c}{dt}\frac{dt}{d\tau}, \quad \frac{dr}{d\tau} = \frac{dr}{dR}\frac{dR}{dt}\frac{dt}{d\tau}.$$

This leads to the dimensionless form of the system:

$$\begin{aligned}
\frac{dn_u}{d\tau} &= a_1 n_u(1-n_u)r - \frac{a_2 n_u n_c}{n_u + a_3 n_r},\\
\frac{dn_r}{d\tau} &= a_4 n_r(1-n_r)r - \frac{a_2 n_r n_c}{n_u + a_3 n_r},\\
\frac{dn_c}{d\tau} &= \frac{a_6 n_u n_c}{n_u + a_3 n_r} - a_7 n_c,\\
\frac{dr}{d\tau} &= r(1-r) - a_8 r n_u - a_9 r n_r,
\end{aligned} \tag{2.3}$$

where

$$a_1 = \frac{r_u}{r_R}, a_3 = \frac{K_r}{K_u}, a_7 = \frac{d}{r_R}, a_2 = \frac{cK_u}{r_R}, a_4 = \frac{r_r}{r_R}, a_6 = \frac{r_c}{r_R}, a_8 = \frac{\alpha_u K_r}{r_R}, a_9 = \frac{\alpha_r K_u}{r_r}.$$

Table 1. Biological significance of variables and parameters.

Variables and Parameters	Biological meaning
$N_u(t)$	Unprotected prey population at time t.
$N_r(t)$	Protected prey population at time t.
$N_c(t)$	Predator population in the free region at time t.
$R(t)$	Resource availability at time t.
$r_u(t)$	Intrinsic growth rate of unprotected prey
$r_r(t)$	Intrinsic growth rate of protected prey
K_u	Carrying capacity of the unprotected prey population.
K_r	Carrying capacity of the protected prey population.
r_c	Growth rate of predators.
d	Death rate of predators.
c	Predation rate coefficient
α_u, α_r	Resource consumption rates for unprotected and protected prey
a_1	The scaled growth rate of prey in the unprotected region
a_2	The resource conversion efficiency
a_3	The relative habitat support of prey population
a_4	The scaled growth rate of prey in the protected region
a_6	The ratio of growth rate of predator-resource
a_7	The ratio of growth rate of death-resource
a_8	Unprotected prey consumption-capacity-growth rate ratio
a_9	Protected prey consumption-capacity-growth rate ratio

3. Analysis of the model system

3.1. Uniqueness, positivity, and boundedness of solution

This section examines the solutions of model system (2.3) with respect to uniqueness, positivity, and boundedness.

Uniqueness

The right-hand side of model system (2.3) is continuous, and within the positive octant domain $\mathcal{Q} = \{(n_u, n_r, n_c, r) \in \mathbb{R}_+^4 : n_u \geq 0, n_r \geq 0, n_c \geq 0, r \geq 0\}$ all partial derivatives of any order are continuous. A system that begins in the non-negative octant will yield a bounded solution. Consequently, model system (2.3) has a unique solution when given a non-negative initial condition.

Positivity of the solution

The positivity of a solution in this context ensures that all variables representing populations or resources (n_u, n_r, n_c, r) remain non-negative for all time $t \geq 0$ if they start from non-negative initial values. This property is essential in ecological models since populations and resources cannot take negative values in realistic scenarios.

Proposition 3.1. *The solution* (n_u, n_r, n_c, r) *of model system (2.3) with positive initial condition* $(n_{u_0}, n_{r_0}, n_{c_0}, r_0)$ *is positive.*

Proof. To demonstrate the positivity of the solution for the given model system, we examine each differential equation:

$$\frac{dn_u}{d\tau} = a_1 n_u (1 - n_u) r - \frac{a_2 n_u n_c}{n_u + a_3 n_r}.$$

Simplifying the terms, we get

$$\frac{dn_u}{d\tau} = \left(a_1 r - \frac{a_2 n_c}{n_u + a_3 n_r} \right) n_u - a_1 r n_u^2,$$
$$\frac{dn_u(\tau)}{d\tau} + f(\tau) n_u(\tau) = -a_1 r n_u^2(\tau),$$

where, $f(\tau) = r a_1 - \dfrac{a_2 n_c}{n_u + a_3 n_r}$, which is Bernoulli form. Therefore, using Bernoulli's differential equation, we obtain

$$n_u(\tau) = \frac{n_{u_0} e^{-\int f(\tau)} d\tau}{1 + n_{u_0} \int e^{\int f(\tau)} a_1 r d\tau},$$

showing that $n_u(\tau) > 0$ for all $t \geq 0$.

Similarly,

$$\frac{dn_r}{d\tau} = a_4 n_r (1 - n_r) r - a_2 \frac{n_r n_c}{n_u + a_3 n_r}.$$

Simplifying the terms, we obtain

$$\frac{dn_r}{d\tau} = \left(a_4 r - \frac{a_2 n_c}{n_u + a_3 n_r} \right) n_r - a_4 r n_r^2,$$
$$\frac{dn_r(\tau)}{d\tau} + h(\tau) n_r = -a_4 r n_r^2,$$

where, $h(\tau) = \left(\dfrac{a_2 n_c}{n_u + a_3 n_r} - a_4 r \right)$.

Solving by Bernoulli's differential equation, we get

$$n_r(\tau) = \frac{n_{r_0} e^{-\int h(\tau)} d\tau}{1 + n_{r_0} \int e^{\int h(\tau)} a_4 r d\tau} > 0 \quad \text{since } n_r \text{ is positive.}$$

The third equation can be written in the form

$$\frac{dn_c}{d\tau} = a_6 \frac{n_u n_c}{n_u + a_3 n_r} - a_7 n_c = \left(\frac{a_6 n_u}{n_u + a_3 n_r} - a_7 \right) n_c.$$

This is in separated form, then integrating both sides, we get

$$n_c(\tau) = n_{c_0} e^{\left(\dfrac{a_6 n_u}{n_u + a_3 n_r} - a_7\right)\tau} > 0 \quad \text{which is positive.}$$

Finally, the fourth equation

$$\frac{dr}{d\tau} = r(1-r) - a_8 r n_u - a_9 r n_r \leq r(1-r).$$

Then, integrating both sides we obtain

$$r(\tau) = \frac{1}{1 + \dfrac{1}{r_0} e^{-\tau}} > 0.$$

Thus, $r(\tau)$ is positive for all $t \geq 0$.

Therefore, for positive initial conditions all solutions of model system (2.3) are positive for all $t \geq 0$. □

Boundedness of solution of the model system

The following proposition establishes the boundedness of the solution for model system (2.3).

Proposition 3.2. *All solutions $(n_u(\tau), n_r(\tau), n_c(\tau), r(\tau))$ of the model system (2.3) with non-negative initial conditions $(n_{u_0}(\tau), n_{r_0}(\tau), n_{c_0}(\tau), r_0(\tau))$ are uniformly bounded within the region*

$$\Lambda = \left\{ (n_u(\tau), n_r(\tau), n_c(\tau), r(\tau)) \in \mathbb{R}_+^4 : 0 < \mathcal{Q}(\tau) \leq \frac{a_1 + a_4}{\phi}, 0 \leq r(\tau) \leq 1 \right\},$$

where, $\mathcal{Q}(\tau) = n_u(\tau) + \dfrac{a_2}{a_6} n_r(\tau) + n_c(\tau)$.

Proof. To show boundedness, we need to confirm that the populations n_u, n_r and n_c do not grow indefinitely but remain within a certain range for all $t \geq 0$.

Define a total population function

$$\mathcal{Q}(\tau) = n_u(\tau) + \frac{a_2}{a_6} n_r(\tau) + n_c(\tau)$$

to represent the sum of the populations of all species. Differentiating $\mathcal{Q}$ with respect to t, we have

$$\frac{d\mathcal{Q}(\tau)}{d\tau} + \phi \mathcal{Q}(\tau) \leq (a_1 + a_4),$$

where, $\phi = min\left\{a_1, a_4, \dfrac{a_2 a_7}{a_6}\right\}$. Therefore, $\mathcal{Q}(\tau) = \dfrac{a_1 + a_4}{\phi} + De^{-\phi\tau}$ where D is a constant. As $\tau \longrightarrow \infty, \mathcal{Q}(\tau) \longrightarrow \dfrac{a_1 + a_4}{\phi}$, that is $0 < \mathcal{Q}(\tau) \leq \dfrac{a_1 + a_4}{\phi}$ which is bounded.

This analysis shows that the predator-prey model, maintains bounded population levels due to intrinsic growth limits, predation, and predator mortality factors.

Therefore, the system's solution is bounded, which is essential for realistic modeling of population dynamics.

Again, to show the boundedness of the differential equation:

$$\frac{dr}{d\tau} = r(1-r) - a_8 r n_u - a_9 r n_r,$$

the terms $a_8 n_u$ and $a_9 n_r$ represent the consumption of the resource by the prey populations n_u and n_r and the term $r(1-r)$ represents logistic growth of the resource r. Thus,

$$\frac{dr}{d\tau} \leq r(1-r).$$

Separation method: $\dfrac{dr}{r(1-r)} \leq d\tau$, we get $r(\tau) = \dfrac{r_0 e^{\tau}}{1 + r_0 e^{\tau}} = \dfrac{r_0}{r_0 + e^{-\tau}}$, which ensures that $r(\tau)$ is initially non-negative.

As $\tau \longrightarrow \infty$, we have $e^{-\tau} \longrightarrow 0$, leading to $r(\tau) \longrightarrow 1$.

Similarly as $\tau \longrightarrow -\infty, e^{-\tau} \longrightarrow \infty$, resulting in $r(\tau) \longrightarrow 0$.

The solution $r(\tau)$ is bounded within the interval $0 \leq r(\tau) \leq 1$ for all t.

Here, one can conclude that all the solutions of the system (2.3) that are initiated in $\mathbb{R}^4_+$ are attracted to the region

$$\Lambda = \left\{ (n_u(\tau), n_r(\tau), n_c(\tau), r(\tau)) \in \mathbb{R}^4_+ : 0 < \mathcal{Q}(\tau) \leq \frac{a_1 + a_4}{\phi}, 0 \leq r(\tau) \leq 1 \right\}.$$

The combined effects of logistic growth, predation, mortality, and resource consumption prevent unbounded growth in any variable, implying that the system remains bounded for all time. Given positive initial conditions, all variables n_u, n_r, n_c and r will stay within biologically feasible limits, ensuring the boundedness of the solution trajectory. This boundedness is crucial for analyzing the model's long-term dynamics, such as persistence or equilibrium behavior. $\square$

3.2. Existence of equilibrium points

To find the equilibrium points of the model (2.3) predator-prey-resource model, we set each of the derivatives $\dfrac{dn_u}{d\tau}, \dfrac{dn_r}{d\tau}, \dfrac{dn_c}{d\tau}, \dfrac{dr}{d\tau}$ to zero. This approach allows us to find points at which the populations of prey in both protected and unprotected regions, the predator, and the resource availability are in a steady state.

The system of equations is:

$$0 = a_1 n_u (1 - n_u) r - a_2 \frac{n_u n_c}{n_u + a_3 n_r}, \tag{3.1}$$

$$0 = a_4 n_r (1 - n_r) r - a_2 \frac{n_r n_c}{n_u + a_3 n_r}, \tag{3.2}$$

$$0 = a_6 \frac{n_u n_c}{n_u + a_3 n_r} - a_7 n_c, \tag{3.3}$$

$$0 = r(1-r) - a_8 r n_u - a_9 r n_r. \tag{3.4}$$

Solving Equation (3.3), we have $n_c = 0$ or $n_u = \dfrac{a_3 a_7}{a_6 - a_7} n_r$. Substituting $n_c = 0$ into equations (3.2) and (3.1), we have $n_r = 0$, or $n_r = 1$ or $r = 0, n_u = 0$, or $n_u = 1$.

If $n_u = 0, n_r = 1$, then $r = 0$, or $r = 1 - a_9$.

If $n_u = 1, n_r = 0$, then $r = 0$, or $r = 1 - a_8$, and if $n_u = 1, n_r = 1$, then $r = 0$, or $r = 1 - a_8 - a_9$.

Generally, we have the following equilibrium point:

- $(0, 0, 0, 0)$ - is the trivial equilibrium point where prey populations, predator and resources are extinct.
- $(0, 1, 0, 1-a_9)$ - prey in the protected region reaches its carrying capacity, and there are no predators or prey in the unprotected region.
- $(1, 0, 0, 1 - a_9)$ -prey in the unprotected region reaches its carrying capacity, and there are no predators or prey in the protected region.
- $(1, 1, 0, 1 - a_8 - a_9)$ - both prey populations reach their carrying capacities, and there are no predators.
- $(n_u^*, n_r^*, n_c^*, r^*)$ - Prey population is at carrying capacity, and there is a balanced population of predators,

where, $n_u^* = \dfrac{a_3a_7(a_1 - a_4)}{a_4(a_7 - a_6) + a_1a_3a_7}, n_r^* = \dfrac{(a_6 - a_7)(a_1 - a_4)}{a_4(a_7 - a_6) + a_1a_3a_7},$

$$n_c^* = \frac{(a_1a_3a_4a_6(a_1 - a_4)(((a_9 - a_3a_8 - 1)a_4 + ((a_8 - 1)a_3 - a_9)a_1)a_7 - a_6)}{(a_7(a_1a_3 + a_4) - a_4a_6)^3},$$

$$r^* = \frac{[(1 + a_8 - a_9)a_4 - ((a_8 - 1)a_3 - a_9)a_1]\, a_7 - a_6(a_4(1 - a_9) + a_1a_9)}{(a_1a_3 + a_4)a_7 - a_4a_6}.$$

To determine the existence of the inner equilibrium point for the given expressions, we must ensure that each expression n_u^*, n_r^*, n_c^*, and r^* is defined, positive, and non-zero by analyzing both the numerators and denominators. Additionally, identifying the intersection (i.e., common factors or conditions) between the numerators and denominators will provide insight into specific constraints for the parameters $a_1, a_3, a_4, a_6, a_7, a_8$ and a_9.

- For n_u^* to be positive, the numerator $a_3a_7(a_1 - a_4)$ must be positive, and the denominator $a_4(a_7 - a_6) + a_1a_3a_7$ must also be positive, which depends on the values of a_1, a_3, a_4, a_6, and a_7.
- For n_r^* to be positive, the numerator $(a_6 - a_7)(a_1 - a_4)$ must be positive, which occurs when $(a_6 - a_7)$ and $(a_1 - a_4)$ have the same sign, and the denominator $(a_7 - a_6)$ must also be positive.
- For n_c^* to be positive, the numerator $a_1a_3a_4a_6(a_1 - a_4)[((a_9 - a_3a_8 - 1)a_4 + ((a_8 - 1)a_3 - a_9)a_1)a_7]$ must be positive, and the denominator $(a_7(a_1a_3 + a_4) - a_4a_6)^3$ must also be positive, which occurs if $a_7(a_1a_3 + a_4) - a_4a_6 > 0$.

Each expression's denominator must remain non-zero to define the equilibrium point. The conditions in the denominators $a_4(a_7 - a_6) + a_1a_3a_7$ and $(a_1a_3 + a_4)a_7 - a_4a_6$ are common requirements across the equilibrium components. Thus, the existence of this equilibrium point hinges on:

(i) Parameter intersection condition: Ensure $a_7(a_1a_3 + a_4) > a_4a_6$ and $a_4(a_7 - a_6) + a_1a_3a_7 > 0$.

(ii) Additional constraints for positivity: $a_1 > a_4, a_7 > a_6$, and suitable values of a_3, a_4, a_6 consistent with non-zero, positive quantities.

If these parameter constraints hold, then all components n_u^*, n_r^*, n_c^*, and r^* are defined, positive, and non-zero. The model equilibrium point thus exists under these parameter values, satisfying both numerator and denominator requirements for each component.

4. Local stability analysis

In this section, we examine the qualitative behavior of system (2.3) by analyzing the local stability of its positive equilibrium points. This analysis offers deeper insight into the model, helping to understand how solution behaviors shift in response to changes in specific parameters. The Jacobian matrix for system (2.3), becomes

$$J(n_u, n_r, n_c, r) = \begin{pmatrix} k_{11} & k_{12} & k_{13} & k_{14} \\ k_{21} & k_{22} & k_{23} & k_{24} \\ k_{31} & k_{32} & k_{33} & 0 \\ k_{41} & k_{42} & 0 & k_{44} \end{pmatrix}, \tag{4.1}$$

where,
$k_{11} = a_1(1-2n_u)r - \dfrac{a_2a_3n_rn_c}{(n_u+a_3n_r)^2}, k_{12} = \dfrac{a_2a_3n_un_c}{(n_u+a_3n_r)^2}, k_{13} = \dfrac{-a_2n_u}{n_u+a_3n_r}$,
$k_{14} = a_1n_u(1-n_u), k_{21} = \dfrac{a_2n_rn_c}{(n_u+a_3n_r)^2}, k_{22} = a_4(1-2n_r)r - \dfrac{a_2n_rn_c}{(n_u+a_3n_r)^2}$,
$k_{23} = \dfrac{-a_2n_r}{n_u+a_3n_r}, k_{24} = a_4n_r(1-n_r), k_{31} = \dfrac{a_3a_6n_rn_c}{(n_u+a_3n_r)^2}, k_{32} = \dfrac{-a_3a_6n_un_c}{(n_u+a_3n_r)^2}$,
$k_{33} = \dfrac{a_6n_u}{n_u+a_3n_r} - a_7, k_{41} = -a_8r, k_{42} = -a_9r, k_{44} = 1 - a_8n_u - a_9n_r$.
We analyze the local stability of the equilibria for system (2.3) in the following propositions.

Proposition 4.1. *The equilibrium point* $E_0^*(0,0,0,0)$ *is unstable.*

Proof. The Jacobian matrix at E_0^* is not defined (or not applicable) due to the collapse of the system at this point. Direct analysis of the system's equations shows that any small positive perturbation from E_0^* leads to growth in one or more state variables. This implies that the system diverges from the equilibrium, and therefore E_0^* is unstable. □

Proposition 4.2. *The equilibrium point* $E_1^*(0,1,0,1-a_9)$ *is unstable with condition* $0 < a_9 < 1$*,* $a_1 > 0$*,* $a_4 > 0$*.*

Proof. The Jacobian matrix of the model system (2.3) at equilibrium point E_1^* substitute into (4.1) is

$$J = \begin{pmatrix} (1-a_9)a_1 & 0 & 0 & 0 \\ 0 & a_4(a_9-1) & \dfrac{-a_2}{a_3} & 0 \\ 0 & 0 & -a_7 & 0 \\ (a_9-1)a_8 & (a_9-1)a_9 & 0 & a_9-1 \end{pmatrix}. \tag{4.2}$$

Then, the eigenvalues of E_1^* are $\lambda_1 = a_1(1-a_9), \lambda_2 = a_4(a_9-1), \lambda_3 = -a_7, \lambda_4 = a_9 - 1$.

Therefore, E_1^* is locally unstable if $0 < a_9 < 1$, $a_1 > 0$, $a_4 > 0$.

The eigenvectors corresponding to eigenvalue $\lambda_1 = a_1(1-a_9), \lambda_2 = a_4(a_9-1), \lambda_3 = -a_7, \lambda_4 = a_9 - 1$, respectively are
$v_1 = \left(\frac{1-a_1}{a_8}, 0, 0, 1\right)^T, v_2 = \left(0, \frac{a_4-1}{a_9}, 0, 1\right)^T,$
$v_3 = \left(0, \frac{1-a_8-a_9}{a_9(a_9-1)}, -\frac{(a_9+a_7-1)(a_4a_9+a_7-a_4)}{a_2a_9(a_9-1)}, 1\right)^T, v_4 = (0,0,0,1)^T.$

The unstable manifold is

$$span\left\{v_4 | 0 < a_9 < 1\right\},$$

in the $n_r r$- plane and the stable manifold is

$$span\left\{v_1, v_2, v_3 | -a_7 < 0\right\},$$

which is $n_u n_c$- plane in the phase space. Therefore, the equilibrium point E_1^* is unstable point with an unstable manifold in $r-$direction and with a stable manifold in $n_u n_r r$-plane.

This biologically meaning prey exists in the protected region only, and resource availability is reduced based on the prey in the protected region. □

Proposition 4.3. *The prey unprotected-resource equilibrium point* $E_2^*(1,0,0,1-a_8)$ *is locally unstable if* $0 < a_8 < 1, a_4 > 0, a_1 > 0$.

Proof. The Jacobian matrix of the model system (2.3) at $E_2^*(1,0,0,1-a_8)$ is

$$J(1,0,0,1-a_8) = \begin{pmatrix} a_1(a_8-1) & 0 & -a_2 & 0 \\ 0 & -a_4(a_8-1) & a_6-a_7 & 0 \\ 0 & 0 & 0 & 0 \\ a_8(a_8-1) & a_9(a_8-1) & 0 & a_8-1 \end{pmatrix}.$$

Then, all eigenvalues are $\lambda_1 = a_1(a_8-1), \lambda_2 = -a_4(a_8-1), \lambda_3 = 0, \lambda_4 = a_8 - 1$. Thus, the system (2.3) at equilibrium point E_2^* is unstable if $0 < a_8 < 1, \quad a_4 > 0, \quad a_1 > 0$. □

Biologically, when n_r and n_c are extinct, the model simplifies to a single prey-resource system where the prey unprotected area (n_u) depends on and is regulated by the resource r, creating a direct relationship between resource availability and prey population. This scenario represents an ecosystem where the unprotected prey thrive independently, limited only by the resource, with no competition or predation constraints.

Proposition 4.4. *The predator free equilibrium point* $E_3^*(1,1,0,1-a_8-a_9)$ *is locally asymptotically stable if*

$$1 > a_8 + a_9, \quad a_6 < a_7(1+a_3), \quad a_1 > 0, \quad a_4 > 0, \tag{4.3}$$

and unstable otherwise.

Proof. The Jacobian matrix of the model system (2.3) at $E_3^*\,(1,1,0,1-a_8-a_9)$ is

$$J\,(1,1,0,1-a_8-a_9)$$

$$=\begin{pmatrix} a_1(a_8+a_9-1) & 0 & \dfrac{-a_2}{a_3+1} & 0 \\ 0 & a_4(a_8+a_9-1) & \dfrac{-a_2}{a_3+1} & 0 \\ 0 & 0 & \dfrac{a_6-a_7(1+a_3)}{a_3+1} & 0 \\ a_8(a_8+a_9-1) & a_9(a_8+a_9-1) & 0 & a_8+a_9-1 \end{pmatrix}.$$

Thus, the eigenvalues of E_3^* are

$\lambda_1 = a_1(a_8+a_9-1), \lambda_2 = a_4(a_8+a_9-1), \lambda_3 = \dfrac{a_6-a_7(1+a_3)}{a_3+1}, \lambda_4 = a_8+a_9-1.$

Hence, the equilibria E_3^* is locally asymptotically stable under condition 4.3, which shows that both prey populations in the unprotected and protected regions reach their carrying capacities and coexist with available resources, with no predators present. □

Proposition 4.5. *The model system (2.3) is locally asymptotically stable around the interior equilibrium point* $E_4^*(n_u^*, n_r^*, n_c^*, r^*)$ *if*

$$b_1>0, \quad b_3>0, \quad b_4>0, \quad b_1b_2b_3-b_3^2-b_1^2b_4>0,$$

where b_1, b_2, b_3 *and* b_4 *are described as below.*

Proof. The Jacobian matrix J of the system (2.3) at the equilibrium point E_4^* is given by

$$J(n_u^*, n_r^*, n_c^*, r^*) = \begin{pmatrix} d_{11} & d_{12} & d_{13} & d_{14} \\ d_{21} & d_{22} & d_{23} & d_{24} \\ d_{31} & d_{32} & d_{33} & 0 \\ d_{41} & d_{42} & 0 & d_{44} \end{pmatrix}, \tag{4.4}$$

where,

$d_{11} = a_1(1-2n_u^*)r^* - \dfrac{a_2a_3n_r^*n_c^*}{(n_u^*+a_3n_r^*)^2}, \;\; d_{12} = \dfrac{a_2a_3n_u^*n_c^*}{(n_u^*+a_3n_r^*)^2}, \;\; d_{13} = \dfrac{-a_2n_u^*}{n_u^*+a_3n_r^*},$

$d_{14} = a_1n_u^*(1-n_u^*), \;\; d_{21} = \dfrac{a_2n_r^*n_c^*}{(n_u^*+a_3n_r^*)^2}, \;\; d_{22} = a_4(1-2n_r^*)r^* - \dfrac{a_2n_r^*n_c^*}{(n_u^*+a_3n_r^*)^2},$

$d_{23} = \dfrac{-a_2n_r^*}{n_u^*+a_3n_r^*}, \;\; d_{24} = a_4n_r^*(1-n_r^*), d_{31} = \dfrac{a_3a_6n_r^*n_c^*}{(n_u^*+a_3n_r^*)^2} \;\; , d_{32} = \dfrac{-a_3a_6n_u^*n_c^*}{(n_u^*+a_3n_r^*)^2},$

$d_{33} = \dfrac{a_6n_u^*}{n_u^*+a_3n_r^*} - a_7, \;\; d_{41} = -a_8r^*, \;\; d_{42} = -a_9r^*, \;\; d_{44} = 1-a_8n_u^*-a_9n_r^*.$

The eigenvalues are obtained from the characteristics equation $det(J(E_4^*)-\lambda I)=0$, which can be written as:

$$\begin{vmatrix} d_{11}-\lambda & d_{12} & d_{13} & d_{14} \\ d_{21} & d_{22}-\lambda & d_{23} & d_{24} \\ d_{31} & d_{32} & d_{33}-\lambda & 0 \\ d_{41} & d_{42} & 0 & d_{44}-\lambda \end{vmatrix} = 0.$$

Now, the characteristic equation of the Jacobian matrix $J(n_u^*, n_r^*, n_c^*, r^*)$ is given by,

$$\lambda^4 + b_1\lambda^3 + b_2\lambda^2 + b_3\lambda + b_4 = 0,$$

where,

$$\begin{aligned}
b_1 =& -(d_{11} + d_{22} + d_{33} + d_{44}),\\
b_2 =&(d_{11}d_{22} + d_{11}d_{33} + d_{11}d_{44} + d_{22}d_{33} + d_{22}d_{44} + d_{33}d_{44} - d_{12}d_{21} - d_{13}d_{31} - d_{23}d_{32}\\
&- d_{24}d_{42} - d_{34}d_{43}),\\
b_3 =&(d_{11}d_{22}d_{33} + d_{11}d_{22}d_{44} + d_{11}d_{33}d_{44} + d_{22}d_{33}d_{44} - d_{12}d_{21}d_{33}\\
&- d_{12}d_{21}d_{44} - d_{13}d_{31}d_{22} - d_{13}d_{31}d_{44} - d_{23}d_{32}d_{11} - d_{23}d_{32}d_{44}\\
&- d_{24}d_{42}d_{11} - d_{24}d_{42}d_{33} + d_{12}d_{23}d_{32} + d_{12}d_{24}d_{42} + d_{13}d_{34}d_{43}\\
&+ d_{23}d_{34}d_{41} + d_{24}d_{41}d_{12}),\\
b_4 =&(d_{11}d_{23}d_{32}d_{44} + d_{12}d_{21}d_{33}d_{44} + d_{12}d_{23}d_{31}d_{42} + d_{11}d_{22}d_{33}d_{44}\\
&+ d_{13}d_{32}d_{41}d_{23} + d_{14}d_{41}d_{22}d_{33} + d_{13}d_{31}d_{22}d_{44} - d_{14}d_{42}d_{31}d_{23} - d_{14}d_{43}d_{32}d_{21}).
\end{aligned}$$

Thus, according to Routh-Hurwitz criteria, the equilibrium points correspond to population levels where the prey (both unprotected and protected), predators, and resources are locally asymptotically stable (balanced) if the sufficient conditions for all roots having negative real part are

$$b_1 > 0, \quad b_3 > 0, \quad b_4 > 0, \quad b_1b_2b_3 - b_3^2 - b_1^2b_4 > 0.$$

□

5. Global stability

To determine the global stability, we need to show that the system converges to a spesific equilibrium point (particularly biologically meaning full) regardless of the initial populations.

Proposition 5.1. *The equilibrium point $E^*(n_u^*, n_r^*, n_c^*, r^*,)$ is globally stable.*

Proof. To examine the behavior of the system in a neighbourhood around the equilibrium point and construct the Lyapunov function to show that the system tends towards the equilibrium, we assume that "resource-free" implies the maximum resource r. This can be modeled by setting $r^* = 1$, which represents maximum resource availability in the logistic growth equation $r(1 - r)$. This implies that $\dfrac{dr(\tau)}{d\tau} = 0$.

A candidate Lyapunov function for the predator-prey system could be:

$$\mathcal{V} = \left(n_u - n_u^* - n_u^* \ln\left|\frac{n_u}{n_u^*}\right|\right) + \left(n_r - n_r^* - n_r^* \ln\left|\frac{n_r}{n_r^*}\right|\right) + \left(n_c - n_c^* - n_c^* \ln\left|\frac{n_c}{n_c^*}\right|\right).$$

The time derivative $\dfrac{d\mathcal{V}}{d\tau}$ is obtained using the system dynamics:

$$\frac{d\mathcal{V}}{d\tau} = \left(\frac{n_u - n_u^*}{n_u}\right)\frac{dn_u}{d\tau} + \left(\frac{n_r - n_r^*}{n_r}\right)\frac{dn_r}{d\tau} + \left(\frac{n_c - n_c^*}{n_c}\right)\frac{dn_c}{d\tau},$$

$$\begin{aligned}\frac{d\mathcal{V}}{d\tau} =& \left(\frac{n_u - n_u^*}{n_u}\right)\left(a_1 n_u(1-n_u) - a_2\frac{n_u n_c}{n_u + a_3 n_r}\right)\\ &- \left[a_1 n_u^*(1-n_u^*) - a_2\frac{n_u^* n_c^*}{n_u^* + a_3 n_r^*}\right]\left(\frac{n_u - n_u^*}{n_u}\right)\\ &+ \left(\frac{n_r - n_r^*}{n_r}\right)\left(a_4 n_r(1-n_r) - a_5 n_r - a_2\frac{n_r n_c}{n_u + a_3 n_r}\right)\\ &- \left[a_4 n_r^*(1-n_r^*) - a_5 n_r^* - a_2\frac{n_r^* n_c^*}{n_u^* + a_3 n_r^*}\right]\left(\frac{n_r - n_r^*}{n_r}\right)\\ &+ \left(\frac{n_c - n_c^*}{n_c}\right)\left(a_6\frac{n_u n_c}{n_u + a_3 n_r} - a_7 n_c - \left[a_6\frac{n_u^* n_c^*}{n_u^* + a_3 n_r^*} - a_7 n_c^*\right]\right).\end{aligned}$$

By distribution we have

$$\begin{aligned}\frac{d\mathcal{V}}{d\tau} =& - a_1\left(1 + \frac{(n_u^* - a_1)}{n_u}\right)(n_u - n_u^*)^2 - a_4\left(1 + \frac{n_r^* a_5 - a_4}{n_r}\right)(n_r - n_r^*)^2\\ &- \frac{a_7}{n_c}(n_c - n_c^*)^2 - \left(\frac{a_2\phi_{n_u}(n_u^*)}{n_u^*} - \frac{a_6\phi_{n_c}(n_c^*)}{n_c^*}\right)\left(\frac{n_u n_c}{n_u + a_3 n_r} - \frac{n_u^* n_c^*}{n_u^* + a_3 n_r^*}\right)\\ &- a_2\left(1 - \frac{n_r^*}{n_r}\right)\left(\frac{n_u n_c}{n_u + a_3 n_r} - \frac{n_u^* n_c^*}{n_u^* + a_3 n_r^*}\right).\end{aligned}$$

Choosing $a_2 = 1, a_6 = \dfrac{n_r^*\phi_{n_u}(n_u^*)}{n_u^*\phi_{n_r}(n_r^*)}a_2$, where

$$\frac{\phi_{n_u}(n_u^*)}{n_u^*} = \left(1 - \frac{n_u^*}{n_u}\right), \frac{\phi_{n_c}(n_c^*)}{n_c^*} = \left(1 - \frac{n_c^*}{n_c}\right),$$

thus, our equation becomes

$$\begin{aligned}\frac{d\mathcal{V}}{d\tau} =& - a_1\left(1 + \frac{(n_u^* - a_1)}{n_u}\right)(n_u - n_u^*)^2 - a_4\left(1 + \frac{n_r^* a_5 - a_4}{n_r}\right)(n_r - n_r^*)^2\\ &- \frac{a_7}{n_c}(n_c - n_c^*)^2 - a_2\left(1 - \frac{n_r^*}{n_r}\right)\left(\frac{n_u n_c}{n_u + a_3 n_r}\right).\end{aligned}$$

Since $\left(1 + \dfrac{(n_u^* - a_1)}{n_u}\right)$ and $\left(1 + \dfrac{n_r^* a_5 - a_4}{n_r}\right)$ are positive, then $\dfrac{d\mathcal{V}}{d\tau} \leq 0$ and $\mathcal{V}(\tau)$ is a lyapunov function. Hence the positive equilibrium point $E_4^*(n_u^*, n_r^*, n_c^*, r^*)$, when $r^* = 1$ of the model system (2.3) is globally asymptotically stable. □

Biologically, predator-prey-resource models tend toward equilibrium, where stable coexistence within the dynamic system supports its long-term stability and function.

5.1. Persistence theorem

We consider the predator-prey population model system (2.3) consisting of n_u - prey in the unprotected area, n_r - prey in the protected area and n_c - predator in the free region. We wish to investigate conditions under which all three population persist. A solution with initial conditions in the positive cone will persist according to our model if there are no $\omega - limit$ points on the boundary of the positive cone (that is on the coordinate axes or planes). Note that each coordinate axis and plane is an invariant set. We assume that the equilibrium point E_1^* is unstable in the $n_r n_c$-plane, if $0 < a_9 < 1$, $a_1 > 0$, $a_4 > 0, a_7 > 0$ and there exists a unique equilibrium E_2^* on the positive $n_u n_c-$ plane, which is unstable if $0 < a_8 < 1, a_4 > 0, a_1 > 0$ in the $n_r n_c-$ plane. Also, an equilibrium point E_3^* is unstable if $a_8 + a_9 < 1, \quad a_6 < a_7(1 + a_3), \quad a_1 > 0, \quad a_4 > 0$ in the $n_u n_c n_r$-plane.

If E_3^* exists, it is assumed to be unique and asymptotically stable in the $n_u n_c n_r$-plane, and E_2^* is assumed to be unstable in the $n_u n_c$-plane. If E_3^* fails to exist, E_2^* is assumed to be asymptotically stable in the $n_u n_c$-plane.

Theorem 5.1. *In addition to the above hypothesis on equilibria, let the following hold:*

- *(i) The right hand side of the model system (2.3) is $C^1 \in (n_u, n_r, n_c)$.*
- *(ii) All solutions of the system (2.3) with non negative initial conditions are bounded in forward time.*
- *(iii) E_1^*, E_2^*, E_3^* (if it exists) are hyperbolic saddle points.*
- *(iv) Interior to each positive coordinate plane there is at most one equilibrium, which, if it exists, is unstable in the positive direction orthogonal to that plane, and around which there are no periodic orbits. Then the model system (2.3) persists.*

Proof. Suppose that $\varphi(\mathcal{X})$ is the orbit through the point in the positive octant $\mathcal{X} = (n_u, n_r, n_c)$ with $n_u > 0, n_r > 0, n_c > 0$. Let $\zeta(\mathcal{X})$ be the $\omega - limit$ set of $\varphi(\mathcal{X})$. Note that by (ii), $\zeta(\mathcal{X})$ is bounded. We claim that the E_1^* does not belong to $\zeta(\mathcal{X})$. If $E_1^* \in \zeta(\mathcal{X})$, then by [22] there exists another point $\xi \in \zeta(\mathcal{X}) \bigcap W^s(E_1^*)$, where $W^s(E_2^*)$ denotes the stable manifold of E_1^* with condition $a_1(1 - a_9) < 0$, $a_4(a_9 - 1) < 0$, $a_7 > 0, a_1 < 0, a_4 > 0$. Since $\zeta(\mathcal{X})$ and $W^s(E_1^*)$ are in the $n_r n_c$-plane, we conclude that $\varphi(\xi)$ is unbounded, which is a contradiction.

Similarly, E_2^* does not belong to $\zeta(\mathcal{X})$.

If $E_2^* \in \zeta(\mathcal{X})$, with conditions $a_8 < 1, a_4 < 0, a_6 < a_7, a_1 > 0$ implying that E_2^* is a stable point and $W^s(E_2^*)$ is in the $n_r n_c$-plane, we conclude that an unbounded orbit lies in the $\varphi(\mathcal{X})$, a contradiction.

In the same way, $E_3^* \notin \zeta(\mathcal{X})$. If $E_3^* \in \zeta(\mathcal{X})$ with the conditions $a_8 + a_9 < 1, \dfrac{a_6 - a_3 a_7}{a_7} < 1, a_1 > 0, a_4 > 0$ implying that E_3^* is a stable point and $W^s(E_3^*)$ is in the $n_u n_r n_c$-plane, again we conclude that an unbounded orbit lies in the $\varphi(\mathcal{X})$, a contradiction. As a result, the model system (2.3) persists, with $\zeta(\mathcal{X})$ residing in the positive octant. Ultimately, because the model system (2.3) is dissipative, only the closed orbits and equilibria constitute the $\omega - limit$ set for solutions on the boundary of $\mathbb{R}_+^3$. □

6. Local bifurcation

A local bifurcation refers to a qualitative change in the behavior of a dynamical system that occurs when a parameter passes through a critical value. This change typically happens in a neighborhood of an equilibrium point or a periodic orbit and is detected through the properties of the system's Jacobian matrix (or other linear stability analysis tools). Local bifurcations help identify critical thresholds at which system dynamics undergo significant transitions. Assuming that the resource r is at its maximum, we consider $r = r_{max} = 1$, meaning resource availability is no longer a limiting factor. In this case, terms involving r in the prey growth rates and the resource equation can be adjusted accordingly. With r set to its maximum $r_{max} = 1$, its dynamics become redundant, so this equation is no longer necessary: $\frac{dr}{dt} = 0$. The dynamics primerly focus on the interactions between prey and predator populations, independent of fluctuating resource availability. They emphasize factors each as predation efficiency, natural mortality, and prey growth rates.

Theorem 6.1. *The model system exhibits saddle node bifurcation at the steady state* $E_2^*(1,0,0)$.

Proof. Two equilibrium points (one stable, one unstable) collide and annihilate each other.

The jacobian matrix at $E_2^*(1,0,0)$ with maximum resource takes the form

$$J_{E_2^*} = \begin{pmatrix} -a_1 & 0 & -a_2 \\ 0 & a_4 & 0 \\ 0 & 0 & a_6 - a_7 \end{pmatrix}.$$

The three eigenvalues of the Jacobian matrix are $\lambda_1 = -a_1, \lambda_2 = a_4, \lambda_3 = a_6 - a_7$, which is a saddle node. By substituting $E_2^*(1,0,0)$ with $a_6 = a_7$ in the Jacobian matrix $J_{E_2^*}$, the characteristic equation has zero eigenvalues.

The eigenvectors V and U associated with zero eigenvalues of matrix J and J^T, respectively are

$$V = (v_1, v_2, v_3)^T = (t_1, 0, 1)^T$$
$$and\ U = (u_1, u_2, u_3)^T = (0, 0, 1)^T,$$

where, $t_1 = \frac{-a_2}{a_6 - a_7 + a_1}$. Let f be the right hand side of the model system

$$f = \begin{pmatrix} a_1 n_u (1 - n_u) r - \frac{a_2 n_u n_c}{n_u + a_3 n_r} \\ a_4 n_r (1 - n_r) r - \frac{a_2 n_r n_c}{n_u + a_3 n_r} \\ \frac{a_6 n_u n_c}{n_u + a_3 n_r} - a_7 n_c \end{pmatrix}.$$

The derivative of the model system with respect to the control parameter a_7 is:

$$f_{a_7} = \begin{pmatrix} 0 \\ 0 \\ -n_c \end{pmatrix}, \quad f_{a_7|_{E_2^*}} = \begin{pmatrix} 0 \\ 0 \\ 0 \end{pmatrix}.$$

$$Df_{a_7}(E_2^*, a_7) = \begin{pmatrix} 0\,0\,0 \\ 0\,0\,0 \\ 0\,0\,0 \end{pmatrix}.$$

The first condition of Sotomayor's theorem is satisfied:

$$U^T f_{a_7}(E_1^*, a_7) = (0,0,1)\begin{pmatrix}0\\0\\0\end{pmatrix} = 0.$$

In addition,

$$Df_{a_7}(E_1^*, a_7)V = \begin{pmatrix}0\;0\;0\\0\;0\;0\\0\;0\;0\end{pmatrix}\begin{pmatrix}t_1\\0\\1\end{pmatrix} = \begin{pmatrix}0\\0\\0\end{pmatrix}, \quad U^T\left[Df_{a_7}(E_1^*, a_7)V\right] = (0,0,1)\begin{pmatrix}0\\0\\0\end{pmatrix} = 0.$$

Computing the third condition of Sotomayor's theorem $U^T\left[D^2 f_{a_7}(E_1^*, a_7)(V,V)\right]$, we use the following:

$$\begin{aligned}&D^2 f(E_1^*, a_7 = a_6)(V,V)\\ =&\frac{\partial^2 f}{\partial n_u^2}v_1^2 + 2\left(\frac{\partial^2 f}{\partial n_u \partial n_r}v_1 v_2 + \frac{\partial^2 f}{\partial n_u \partial n_c}v_1 v_3 + \frac{\partial^2 f}{\partial n_r \partial n_c}v_2 v_3\right)\\ &+\frac{\partial^2 f}{\partial n_r^2}v_2^2 + \frac{\partial^2 f}{\partial n_c^2}v_3^2 + \ldots.\end{aligned} \tag{6.1}$$

with,

$$\begin{aligned}f_1 =& a_1 n_u(1-n_u)r - \frac{a_2 n_u n_c}{n_u + a_3 n_r},\\ f_2 =& a_4 n_r(1-n_r)r - \frac{a_2 n_r n_c}{n_u + a_3 n_r},\\ f_3 =& \frac{a_6 n_u n_c}{n_u + a_3 n_r} - a_7 n_c.\end{aligned}$$

After some calculation, we have

$$D^2 f(E_1^*, a_7)(V,V) = \begin{pmatrix}D^2 f_1(E_1^*, a_7)(V,V)\\ D^2 f_2(E_1^*, a_7)(V,V)\\ D^2 f_3(E_1^*, a_7)(V,V)\end{pmatrix} = \begin{pmatrix}t_{11}\\t_{21}\\t_{31}\end{pmatrix},$$

where,

$$\begin{aligned}D^2 f_1(E_1^*, a_7)(V,V) &= \left(-2a_1 + \frac{2a_2 a_3 n_c}{(n_u + a_3 n_r)^3}\right)t^2 + 2\left(\frac{2a_2^2}{(n_u + a_3 n_r)^2(a_6 - a_7 + a_1)}\right),\\ D^2 f_2(E_1^*, a_7)(V,V) &= \left(\frac{-a_2 n_r n_c}{(n_u + a_3 n_r)^3}\right)t^2 - \left(\frac{2a_2^2 n_r}{(n_u + a_3 n_r)^2(a_6 - a_7 + a_1)}\right),\\ D^2 f_3(E_1^*, a_7)(V,V) &= \left(\frac{-2a_3 a_6 n_r n_c}{(n_u + a_3 n_r)^3}\right)t^2 - \left(\frac{2a_2 a_3 a_6 n_r}{(n_u + a_3 n_r)^2(a_6 - a_7 + a_1)}\right).\end{aligned}$$

$$U^T\left[D^2 f(E_1^*, a_7)(V,V)\right] = (0,0,1)\begin{pmatrix}t_{11}\\t_{21}\\t_{31}\end{pmatrix} = t_{31} \neq 0.$$

By computation we have,

$$U^T f_{a_7}(E_1^*, a_7) = 0, U^T \left(Df_{a_7}(E_1^*, a_7)V\right) = 0, U^T \left[D^2 f(E_1^*, a_7)(V, V)\right] \neq 0.$$

Thus, the systems satisfy the necessary conditions of a saddle node bifurcation around the coexistence fixed point E_2^* at the threshold $a_7 = a_6$ as outlined by Sotomayor's theorem [23]. The equilibrium point E_2^* in the biological system corresponds to a saddle node bifurcation, thereby constituting a critical threshold where infinitesimal perturbations of system parameters may cause significant behavioral transitions.

$\square$

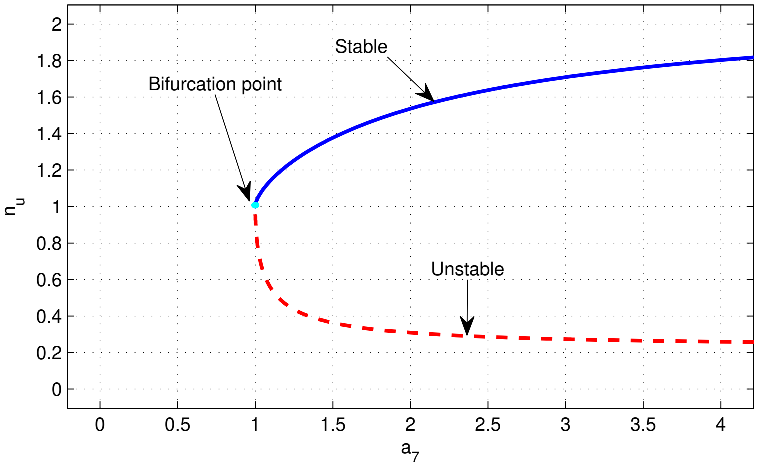

Figure 1. Bifurcation diagram

Figure 1 shows that the rate at which the predator converts prey consumption into its population growth. A bifurcation at $a_7 = a_6$ implies that changes in this parameter lead to a qualitative shift in the dynamics of the system. The solid blue curve represents a stable equilibrium, meaning that under these conditions, the prey population in the unprotected region remains at a steady level. The dashed red curve represents an unstable equilibrium, indicating that slight disturbances in prey population at these levels will result in a shift away from equilibrium, potentially leading to extinction or explosive growth. This is a critical threshold where the system's dynamics qualitatively change. For values of a_6 below a_7, the prey population may have a lower stable state or even face collapse due to high predator consumption. For values above a_7, the prey population stabilizes at a higher level, potentially due to a reduced predation rate or increased prey reproduction. Conservation measures, such as creating a reserved region where prey can escape predation, might help maintain prey populations above the bifurcation threshold.

Theorem 6.2. *The system described by Equation (2.3) undergoes a transcritical bifurcation around the equilibrium point* $E_3^*(1, 1, 0)$ *when the system parameters meet the condition* $a_6 = a_7(1 - a_3)$*. Here,* $a_6 = a_7(1 - a_3)$ *serves as the bifurcation parameter.*

Proof. We also apply Sotomayor's theorem [23,24] to demonstrate the occurrence of a transcritical bifurcation under the transversality condition $a_6 = a_7(1-a_3)$. The

Jacobian matrix at the equilibrium point $E_3^*(1,1,0)$ is expressed as:

$$J_{E_3^*} = \begin{pmatrix} -a_1 & 0 & \dfrac{-a_2}{1+a_3} \\ 0 & -a_4 & \dfrac{-a_2}{1+a_3} \\ 0 & 0 & \dfrac{-a_3a_7 - a_6 + a_7}{1+a_3} \end{pmatrix}.$$

The eigenvalues of the Jacobian matrix are

$$\lambda_1 = -a_1, \lambda_2 = -a_4, \lambda_3 = \frac{-a_6 + a_7(1-a_3))}{1+a_3}.$$

By substituting E_3^*, the characteristic equation has zero eigenvalue at $a_6 = a_7(1 - a_3)$. The eigenvectors $W_1 = (w_1, w_2, w_3)^T$ and $W_2 = (w_1^*, w_2^*, w_3^*)^T$ associated with zero eigenvalues of matrix J and J^T, respectively, are $W_1 = (q_1, q_2, 1)^T$ and $W_2 = (0,0,1)^T$, where, $q_1 = \dfrac{-a_2}{a_3(a_1 - a_7) + a_4 + a_6 - a_7}, q_2 = \dfrac{a_2}{a_3(a_1 - a_7) + a_4 + a_6 - a_7}$. Moreover,

$$f_{a_6} = \begin{pmatrix} 0 \\ 0 \\ \dfrac{n_u n_c}{n_u + a_3 n_r} \end{pmatrix} = f_{a_6|_{E_3^*(1,1,0)}} = \begin{pmatrix} 0 \\ 0 \\ 0 \end{pmatrix}.$$

$$Df_{a_6}(E_3^*(1,1,0)) = \begin{pmatrix} 0 & 0 & 0 \\ 0 & 0 & 0 \\ 0 & 0 & \dfrac{1}{1+a_3} \end{pmatrix}.$$

The first condition of Sotomayor's theorem is

$$W_2^T f_{a_6}(E_3^*(1,1,0)) = (0,0,1) \begin{pmatrix} 0 \\ 0 \\ 0 \end{pmatrix} = 0,$$

$$W_2^T[Df_{a_6}(E_3^*(1,1,0))W_1] = (0,0,1) \begin{pmatrix} 0 & 0 & 0 \\ 0 & 0 & 0 \\ 0 & 0 & \dfrac{1}{1+a_3} \end{pmatrix} \begin{pmatrix} 0 \\ 0 \\ \dfrac{1}{1+a_3} \end{pmatrix} = \frac{1}{(1+a_3)^2}.$$

Evaluating $D^2f(E_1^*, a_7)(V,V)$, using Equation 6.1, we get

$$D^2f(E_1^*, a_7)(V,V) = \begin{pmatrix} D^2f_1(E_1^*, a_7)(W_1, W_1) \\ D^2f_2(E_1^*, a_7)(W_1, W_1) \\ D^2f_3(E_1^*, a_7)(W_1, W_1) \end{pmatrix} = \begin{pmatrix} f_{11} \\ f_{21} \\ f_{31} \end{pmatrix},$$

where,

$$\begin{aligned}
f_{11} &= \left(-2a_1 + \frac{2a_2a_3n_c}{(n_u+a_3n_r)^3}q_1^2\right) + 2\left(\frac{2a_2a_3}{(n_u+a_3n_r)^3}q_1q_2 - \frac{a_2n_r}{(n_u+a_3n_r)^2}q_1\right)\\
&\quad - \frac{2a_2a_3^2}{(n_u+a_3n_r)^2}q_2^2 - \frac{a_2}{n_u+a_3n_r},\\
f_{21} &= -\left(\frac{a_2n_rn_c}{(n_u+a_3n_r)^3}q_1^2\right) + 2\left(\frac{2a_2n_un_c}{(n_u+a_3n_r)^3}q_1q_2 + \frac{a_2n_r}{(n_u+a_3n_r)^2}q_1\right)\\
&\quad - \frac{a_2n_u}{(n_u+a_3n_r)^2}q_3 + \left(-2a_4 + \frac{2a_3n_un_c}{(n_u+a_3n_r)^2}\right)q_2^2,\\
f_{31} &= -\left(\frac{2a_3a_6n_rn_c}{(n_u+a_3n_r)^3}q_1^2\right) + 2\left(\frac{a_3a_6(1-a_3)n_rn_c}{(n_u+a_3n_r)^3}q_1q_2 + \frac{a_3a_6n_r}{(n_u+a_3n_r)^2}q_1\right)\\
&\quad + \frac{2a_3^2a_6n_un_c}{(n_u+a_3n_r)^3}q_2^2.
\end{aligned}$$

Then,

$$W_2^T\left[D^2f(E_1^*,a_7)(W_1,W_1)\right] = (0,0,1)\begin{pmatrix} f_{11}\\ f_{21}\\ f_{31}\end{pmatrix} = f_{31} \neq 0.$$

One obtains,

$$W_2^T f_{a_6}(E_3^*,a_6) \neq 0, W_2^T\left(Df_{a_6}(E_3^*,a_6)W_1\right) \neq 0, W_2^T\left[D^2f(E_3^*,a_6)(W_1,W_1)\right] \neq 0,$$

which means that when $a_6 = a_7(1-a_3)$, the transcritical bifurcation occurs at E_3^*. The condition $a_6 = a_7(1-a_3)$ signifies a critical threshold at which the system undergoes a transcritical bifurcation at the equilibrium point $E_3^*(1,1,0)$. Biologically, this implies that when the predator's consumption rate a_6 reaches this critical value, the population dynamics shift, potentially altering the stability of equilibria and leading to changes in the persistence or extinction of species. Thus, the bifurcation condition highlights the delicate balance between the population feeding capacity and mortality, determining whether the population can sustain itself or faces extinction. □

Changes in predation efficiency and mortality rates could destabilize or stabilize predator populations as illustrated in Figure 2.

Biologically, predator-prey coexistence equilibria may lose stability, shifting to extinction or dominance scenarios. The bifurcation analysis provides insights into how prey competition and predator-prey interactions shape the ecological balance. At the bifurcation point, the system may transition to oscillations, coexistence, or extinction scenarios, emphasizing the delicate interplay of competition, predation, and resource constraints.

7. Numerical method

This section describes the numerical methods used to model system (2.3). The system's behavior is analyzed with MATLAB's variable-step Runge-Kutta solver,

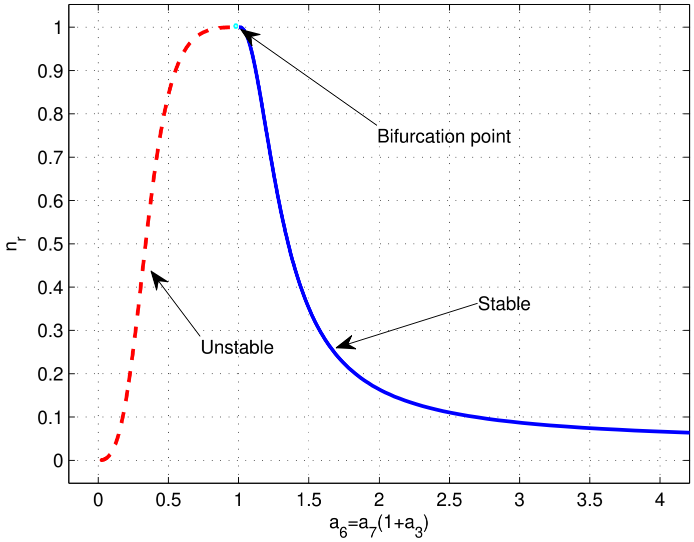

Figure 2. Bifurcation trajectories

ode45, yielding simulation results that validate the analytical findings and enhance our understanding of the system's dynamics. Stability analysis is conducted using the Lyapunov function and Hurwitz criteria, while the Lipschitz condition is employed to establish the existence and uniqueness of solutions for the model system. In the following subsections, numerical solutions for system (2.3) are provided, with a focus on varying one parameter at a time. This parameter-specific analysis highlights how changes in parameter values affect the system's behavior.

7.1. Numerical simulation

This study presents simulation results from analyzing model system (2.3) using the ode45 solver. These numerical outcomes not only validate our analytical findings but also offer a more detailed understanding of the model's dynamic properties. In subsequent sections, we explore the numerical solutions of model system (2.3) by varying one parameter at a time, based on the information provided within the system. This approach enables a systematic investigation into how changes in parameter values impact the system's behavior. The interaction of ecological parameters determines whether a system reaches equilibrium, undergoes oscillations, or collapses. For instance, high predation rates, low prey growth rates, and resource scarcity are more likely to induce population cycles or crashes. On the other hand, incorporating factors such as predator switching, functional response saturation, and resource availability can enhance system stability and promote more sustainable predator-prey dynamics. Parameter estimation for the remaining variables was conducted by enforcing the conditional requirements detailed in preceding sections. The resulting parametric values are documented in Table 2 [25].

Figure 3 illustrates the interior equilibrium scenario of model system (2.3), supporting the global stability proposed in Proposition 5.1 by demonstrating the tra-

Table 2. The system parameter values

System Parameters	Parameter value(s)	Reference
r_u, r_c, c, d	0.5, 0.8, 0.5, 0.75	[18]
r_r, γ	0.58, 2.0	[25]
K_u	0.8	
r_r	0.58	[26]
K_r, α_u, α_r	1.0, 0.3, 0.2	Estimation

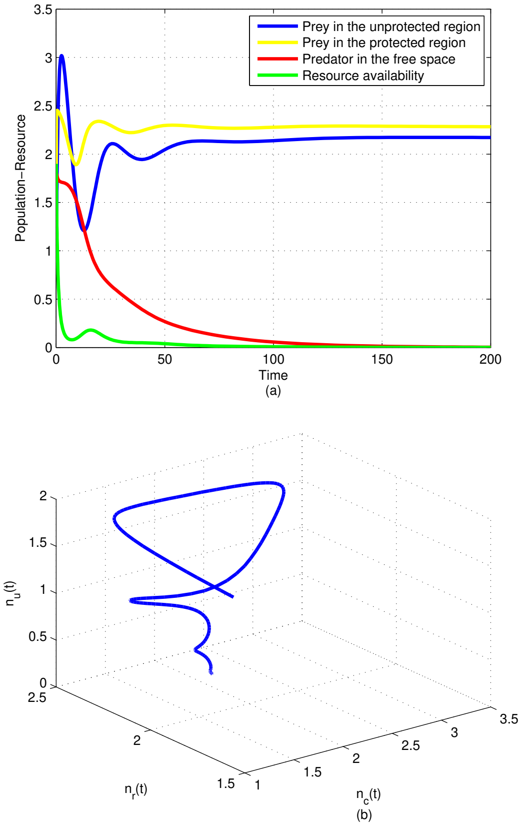

Figure 3. (a) shows the time series plot of the model system that converges to the$(1.00, 1.56, 1.818, 1.9)$, while (b) is the trajectories of a system of the equations over time which provides stability of this point.

jectory behavior. This scenario reflects a state in which all three species can coexist sustainably, provided resources remain available, while population levels will decline with reduced resource availability. The time series plot Figure 3(a) illustrates the dynamic interactions among prey populations in protected and unprotected regions, predators in free space, and resource availability. Initially, the prey population in the unprotected region (blue) exhibits a rapid decline due to intense predation pressure, followed by stabilization as the system reaches equilibrium. In contrast, prey in the protected region (yellow) experiences a brief fluctuation before settling at a stable level, benefiting from reduced predation. The predator population (red) initially rises but quickly declines due to diminishing prey availability, eventually stabilizing at a lower equilibrium. Resource availability (green) remains relatively constant after an initial fluctuation, indicating a balance between consumption and replenishment. The three dimensional phase trajectory plot Figure 3(b) provides insight into the system's long term stability. The trajectories suggest a convergent dynamic, where the system stabilizes at a fixed point, confirming the existence of an equilibrium state. The initial oscillatory behavior reflects transient fluctuations before the populations settle into a stable coexistence. This behavior highlights the ecological importance of spatial heterogeneity and resource distribution in maintaining population stability, demonstrating how protected regions can buffer prey populations from excessive predation, ultimately supporting the persistence of both prey and predator species.

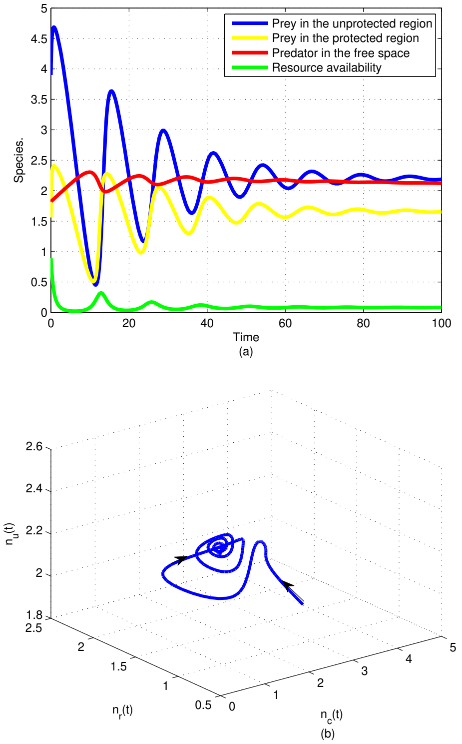

Figure 4. (a) shows the time series plot of the model system that converges to the $(3.9, 1.56, 1.818, 0.9)$, while (b) is the trajectories of a system of the equations over time which provides stability of this point.

Figure 4 above illustrates that oscillations settle down into a stable situation and all three species persist in stable position and the resource availability decreases. Figure 4 illustrates the coexistence of predator and prey populations at equilibrium, shaped by spatial heterogeneity and resource availability. The time series plot Figure 4(a) shows initial oscillations in prey populations, particularly in the unprotected region (blue), due to high predation pressure before stabilizing. The protected region (yellow) supports a more stable prey population, while predators (red) fluctuate before settling at a lower equilibrium level. Resource availability (green) remains relatively stable, indicating a balance between consumption and replenishment. The phase trajectory plot Figure 4(b) confirms the system's convergence toward a stable equilibrium, highlighting the role of spatial refuges and resource distribution in sustaining predator-prey coexistence.

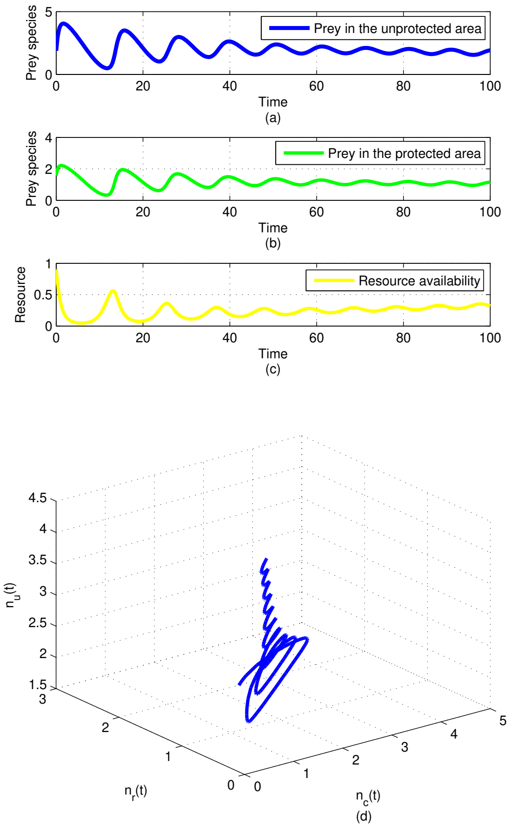

Figure 5. Stability of prey-resource and predator free scenario

Figure 5 illustrates the dynamics of ecosystems with spatial separation (protected versus unprotected regions) of prey populations and resource constraints at the maximum resource availability $r = 1$ with initial value $(0.42, 0.40, 0.42)$, emphasizing the critical roles of resource availability and predation dynamics in shaping population outcomes. In this context, resources are assumed to reach a maximum availability level of one, and the predator population becomes extinct ($n_c = 0$). Initially, as resource availability declines, the prey population increases and persists. Over time, as the prey population decreases, resource availability gradually recovers.

Figure 6 illustrates that initially, the predator-prey population decreases, while the resource population increases due to the absence of predators and prey. After some time, the prey population starts to grow and approaches its carrying capacity, leading to a decline in both the predator population and resource availability.

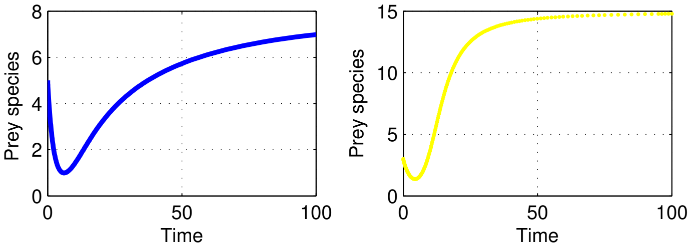

(a) Prey in the unprotected region (b) Prey in the protected region

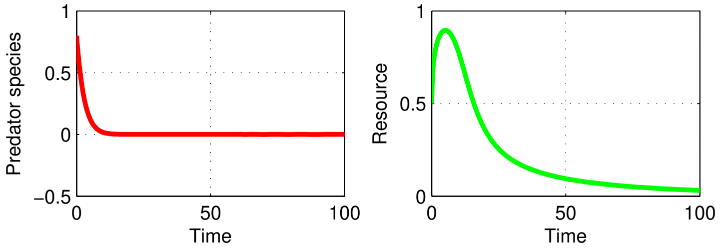

(c) Predator species (d) Resource availability

Figure 6. Existence of populations at the initial condition $(5.00, 3.00, 0.2, 0.4)$ with parameter values $\mu = 5.0, c = 0.5, d = 0.75, \alpha_u = 4.0, \gamma = 2.0$

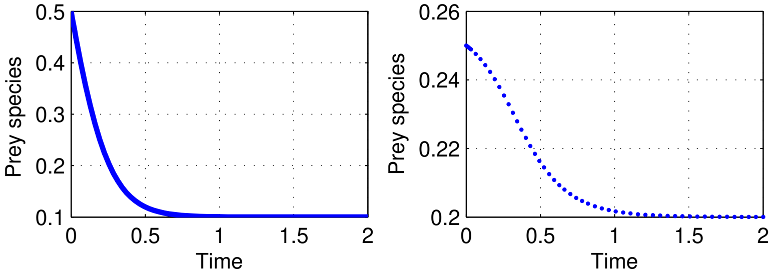

(a) Prey in the unprotected area (b) Prey in the protected area

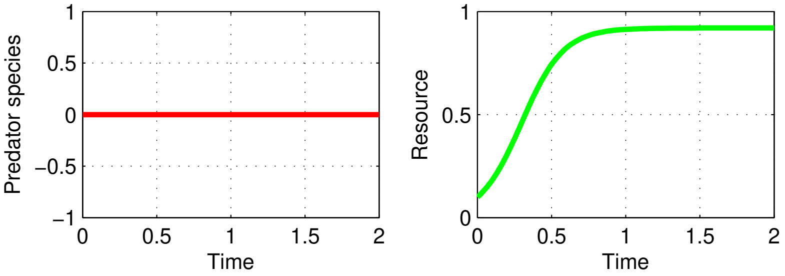

(c) Predator species (d) Resource availability

Figure 7. Stability of populations at the equilibrium point $(1.0, 0.25, 0.0, 1.0)$ with parameter $c = 0.005, \alpha_u = 0.4, \alpha_r = 0.3, d = 0.5$

Figure 7 depicts a gradual increase in resource availability due to the absence of predator populations, accompanied by a steady decline in prey populations in both the unprotected and protected regions. This behavior, consistent with Proposition 4.4, demonstrates population instability under certain conditions.

7.2. Impact of resource availability on population dynamics

Resource availability r plays a critical role in regulating the dynamics of prey and predator populations in the given model. It directly influences the growth rates of both prey populations N_u and N_r, as their logistic growth terms are scaled by $\dfrac{R}{R_{max}}$. This means that higher resource availability promotes faster prey growth, while lower availability limits it. Predation efficiency is also indirectly affected, as sufficient resources sustain prey populations, enabling predation. Conversely, reduced resource levels can lead to diminished prey densities, thereby lowering predation rates. The predator population N_c depends on prey availability, which is inherently tied to R, so insufficient resources may cascade through the system, limiting predator growth and survival. Additionally, the resource dynamics include depletion terms $\alpha_u N_u R$ and $\alpha_r N_r R$, representing the consumption of resources by prey populations. High prey densities can deplete resources, creating feedback loops that regulate population sizes. Finally, resource availability indirectly determines the carrying capacity of the prey populations, with declines in R potentially leading to reduced carrying capacities and population crashes. Thus, resource availability is a central factor driving the interactions and stability of prey and predator populations in this ecological model. The importance of the model lies in its ability to provide insights into the complex interactions between prey populations, predator populations, and resource availability in ecological systems. By incorporating factors such as logistic growth, predation, and resource dynamics, the model captures realistic ecological processes that help in understanding population stability, coexistence, and oscillatory behavior. Specifically, the inclusion of protected and unprotected prey regions allows for the analysis of spatial heterogeneity, while the explicit role of resource availability highlights its critical influence on population growth and predator-prey interactions. This model is essential for identifying key parameters and mechanisms that promote ecological balance and can be used to predict the impact of environmental changes, such as resource depletion or habitat modifications. Furthermore, it serves as a foundation for exploring conservation strategies, such as the role of prey refuges and sustainable resource management, to ensure species coexistence and ecosystem stability.

8. Discussion

In this paper, we have explored the dynamical behavior of a predator-prey model that incorporates resource availability as a factor influencing both predator and prey populations. The interaction between the predator and prey is governed by a Holling type II functional response, which is adapted to include the effect of resource availability. As highlighted by [27, 28], the Holling type II response function is widely used to model predator-prey interactions due to its realistic representation of food limitations. The novelty of this work lies in analyzing such predator-prey interactions under the influence of resource availability, providing a more realistic perspective on ecosystem dynamics. We derived the criteria for the existence of biologically meaningful equilibrium points and conducted a detailed stability analysis.

The study underscores the complex interplay between spatial heterogeneity, resource availability, and initial conditions in predator-prey interactions. These insights have important implications for conservation efforts, highlighting the necessity of careful resource management to support biodiversity and ensure species persistence. Figure 6 illustrates the dynamics of a predator-prey system with resource constraints, initialized at equilibrium point $E^*(5.0, 3.0, 0.2, 0.4)$ and governed by parameters in Table 2. Under these conditions, prey populations flourish, reaching stable levels in both protected and unprotected regions, while the predator population collapses, potentially leading to extinction. Simultaneously, resource availability declines significantly. These results emphasize the critical role of initial conditions and parameter values in shaping ecological dynamics, influencing population growth, decline, and extinction.

Figure 3 demonstrates that a decline in resources, caused by factors such as deforestation, environmental degradation, or mismanagement, leads to the decline of both predator and prey populations. This underscores the vital role of resource availability in maintaining ecological balance and ensuring the sustainability of populations. The primary advantage of model system (2.1) lies in its ability to capture the intricate interplay between prey populations, predator dynamics, and resource availability in both unprotected and protected regions. By distinguishing between prey in protected and unprotected areas, the model accounts for spatial heterogeneity and the potential refuge effect that can reduce predation pressure in certain habitats. The inclusion of resource dynamics ensures that the model reflects the critical role of resource availability in regulating population growth and interactions. Moreover, Figure 4 illustrates the stable coexistence of predator and prey populations at equilibrium point $E(3.9, 1.56, 1.818, 0.9)$. This equilibrium is achieved through the interplay of spatial heterogeneity and resource availability, where protected regions buffer prey from over predation. The time series Figure 4(a) shows initial population fluctuations converging towards stability, while the phase space representation Figure 4(b) confirms this with a trajectory spiraling into a single point. This model highlights the ecological importance of spatial heterogeneity and resource distribution in maintaining population stability and enabling the long term persistence of both predator and prey species. Additionally, the nonlinear terms incorporate realistic ecological processes, such as logistic growth and predation saturation, while allowing the examination of factors like predator-prey interaction and resource limitation. This comprehensive framework provides a versatile tool for studying stability, coexistence, and oscillatory behavior in ecological systems, making it particularly valuable for understanding population dynamics in complex environments.

9. Conclusion

Contemporary research in theoretical ecology has advanced through the exploration of modern concepts addressing ecological challenges, grounded in foundational models such as the predator-prey, food chain, and competitive species models [29, 30]. Predator-prey interaction mechanisms are central to understanding the dynamics of ecological systems. This study examines a modified version of the model system in [18], incorporating resource availability to support predator-prey populations. Analyzing the model under specified conditions provides valuable insights into the potential behaviors and stability of this predator-prey-resource system. This model captures dynamics involving two spatially distinct prey populations, one predator population, and a shared resource. The dynamics of resource R are crucial, as they must balance prey consumption rates to sustain equilibrium. High consumption rates by N_u and N_r can deplete the resource R, influencing the carrying capacities of each prey population. At maximum resource availability ($R = 1$), the system achieves peak potential for prey growth, which may elevate predation pressure as prey populations increase, subsequently affecting the predator N_c. In this scenario, all species persist with resources maintained in a balanced state between prey consumption and natural replenishment. Prey populations are regulated solely by the availability of resources, which can result in higher equilibrium densities for prey. This balance maximizes the growth potential for prey, which, in turn, can lead to increased predation and potentially higher equilibrium levels for predators, provided consumption remains in balance. Thus, the model indicates that a stable predator-prey-resource system depends on a dynamic equilibrium where resource availability supports prey growth without leading to overconsumption by predators. The bifurcation analysis reveals that the ecological balance of the system is significantly influenced by prey competition and predator-prey interactions, leading to various dynamic outcomes at bifurcation points, including oscillations, coexistence, and extinction.

In this study, the Holling type-II functional response model has been extended to incorporate the influence of resource availability on prey populations, reflecting their ecological significance [12]. Beyond theoretical insights, this model provides practical implications for resource management and ecological conservation. Understanding the thresholds of resource availability and consumption can inform conservation strategies, ensuring sustainable predator-prey coexistence. The findings highlight the importance of maintaining habitat resources at levels that prevent population collapses and ecosystem imbalances. By applying this model, conservationists can develop strategies to regulate resource use, mitigate overexploitation, and enhance biodiversity sustainability. For further study, model (2.1) could be extended by introducing a time delay, spatial diffusion, and stochastic effects to better understand the stability of the system. This addition would allow researchers to analyze how delayed responses in resource availability or predation, as well as spatial dispersal mechanisms, affect long-term population dynamics. These extensions can offer deeper insights into ecological resilience and the effects of environmental variability on species interactions.

References

[1] Sahoo, B., Das, B., Samanta, S, *Dynamics of harvested-predator-prey model: role of alternative resources*. Modeling Earth Systems and Environment, 2016, 2, 1–12.

[2] Sardar, A., Hanif, M., Asaduzzaman, M., Biswas, M., *Mathematical analysis of the two species lotka-volterra predator-prey inter-specific game theoretic competition model*. Advanced Modeling and Optimization, 2016, 18(2), 231–242.

[3] Berryman, A.A., *The orgins and evolution of predator-prey theory*. Ecology, 1992, 73(5), 1530–1535.

[4] Brauer, F., Castillo-Chavez, C., Castillo-Chavez, C., *Mathematical Models in Population Biology and Epidemiology*, 2012, vol. 2(40). Springer.

[5] Boyce, M.S.,*Modeling predator-prey dynamics. Research techniques in animal ecology.* Columbia University Press, 2000, New York, USA, 253–287.

[6] Lv, Y., Du, Z. *Existence and global attractivity of a positive periodic solution to a lotka-volterra model with mutual interference and holling iii type functional response.* Nonlinear analysis: real world applications, 2011, 12(6), 3654–3664.

[7] Castellanos, V., Chan-L'opez, R.E., *Existence of limit cycles in a three level trophic chain with lotka-volterra and holling type ii functional responses.* Chaos, Solitons & Fractals, 2017, 95, 157–167.

[8] Nair, P.R., *Ecophysiology and Food Web Dynamics of Spring Ecotone Communities in the Edwards Aquifer, USA.* Texas State University-San Marcos, 2019.

[9] Decocq, G., Regnault, P., Lenoir, J., Paccaut, F., Di Menza, L., Delvoye, G., Janvresse, E., Closset-Kopp, D., Goubet, O., *Modelling plant community dynamics in changing forest ecosystems: a review.* Botany Letters, 2023, 170(4), 541–564.

[10] Farahbakhsh, I., Bauch, C.T., Anand, M., *Modelling coupled human-environment complexity for the future of the biosphere: strengths, gaps and promising directions.* Philosophical Transactions of the Royal Society B, 2022, 377(1857), 20210382.

[11] Justus, J., *The Philosophy of Ecology: An Introduction.* Cambridge University Press, 2021.

[12] Das, A., Mandal, S., Roy, S.K., *Bifurcation analysis within a modified may-holling-tanner prey-predator system via allee effect and harvesting on predator.* Numerical Algebra, Control and Optimization, 2025, 15(3): 800–822.
doi: 10.3934/naco.2024043

[13] Jana, A., Kumar Roy, S. *Holling-tanner prey-predator model with beddington-deangelis functional response including delay.* International Journal of Modelling and Simulation, 2022, 42(1), 86–100.

[14] Bolnick, D.I., Preisser, E.L., *Resource competition modifies the strength of trait-mediated predator-prey interactions: A meta-analysis.* Ecology, 2005, 86(10), 2771–2779.

[15] Nevai, A.L., Van Gorder, R.A., *Effect of resource subsidies on predator-prey population dynamics: a mathematical model.* Journal of biological dynamics, 2012, 6(2), 891–922.

[16] Cao, Q., Chen, G., Yang, W., *The impact of fear effect on the dynamics of a delayed predator-prey model with stage structure.* International Journal of Biomathematics, 2023, 16(08), 2250139.

[17] Hu, D., Li, Y., Liu, M., Bai, Y., *Stability and hopf bifurcation for a delayed predator-prey model with stage structure for prey and ivlev-type functional response.* Nonlinear Dynamics, 2020, 99, 3323–3350.

[18] Wayesa, N.N., Obsu, L.L., Dawed, M.Y., *Analysis of predator-prey model with inclusion of temperature variability in prey refugees.* Journal of Applied Mathematics, 2024, 2024(1), 5138320.

[19] Gebreyohannes, G.T., *Prey switching in predator prey model.* PhD thesis, Stellenbosch University, South Africa 2016.

[20] Pepi, A., Grof-Tisza, P., Holyoak, M., Karban, R., *As temperature increases, predator attack rate is more important to survival than a smaller window of prey vulnerability.* Ecology, 2018, 99(7), 1584–1590.

[21] Wayesa, N.N., Obsu, L.L., Dawed, M.Y., *Predator-prey population dynamics with time delay and prey refuge effects.* Modeling Earth Systems and Environment, 2025, 11(2), 142.

[22] Butler, G., Freedman, H.I., Waltman, P. *Uniformly persistent systems.* Proceedings of the American Mathematical Society, 1986, 425–430.

[23] Perko, L. *Differential Equations and Dynamical Systems, 2013, vol. 7.* Springer.

[24] Kumar, A., Dubey, B., *Stability and bifurcation of a prey-predator system with additional food and two discrete delays.* Computer Modeling in Engineering & Sciences, 2021, 126(2), 505–547.

[25] Jana, A., Roy, S.K., *Harvesting in a toxicated intraguild delayed fishery model with variable carrying capacity.* Computational and Applied Mathematics, 2022, 41(8), 414.

[26] Jana, A., Roy, S.K., *Fostering roles of super predator in a three-species food chain.* International Journal of Dynamics and Control, 2023, 11(1), 78–93.

[27] Molla, H., Sabiar Rahman, M., Sarwardi, S., *Dynamics of a predator-prey model with holling type ii functional response incorporating a prey refuge depending on both the species.* International Journal of Nonlinear Sciences and Numerical Simulation, 2019, 20(1), 89–104.

[28] Mondal, B., Rahman, M.S., Sarkar, S., Ghosh, U., *Studies of dynamical behaviours of an imprecise predator-prey model with holling type ii functional response under interval uncertainty.* The European Physical Journal Plus, 2022, 137(1), 1–20.

[29] Mandal, G., Ali, N., Guin, L.N., Chakravarty, S., *Impact of fear on a tritrophic food chain model with supplementary food source.* International Journal of Dynamics and Control, 2023, 11(5), 2127–2160.

[30] Lv, S., Zhao, M., *The dynamic complexity of a three species food chain model.* Chaos, Solitons & Fractals, 2008, 37(5), 1469–1480.